A Study on MIMO Mobile-To-Mobile Wireless Fading Channel Models

MSc Luis Alfredo Mateos Guzmán, Dr Cheng-Xiang Wang, and MSc Xiang Cheng

***Abstract*— Mobile-to-Mobile (M2M) communications applications can be seen in mobile ad-hoc networks, wireless sensor networks, and intelligent transport systems, these systems require direct communication between a mobile transmitter and a mobile receiver over a wireless medium. Such Mobile-to-Mobile communication systems differ from the conventional cellular radio systems, where the Base Station is stationary and only the Mobile Station is moving.**

The employment of multiple antennas at both the transmitter and receiver, known as Multiple Input Multiple Output (MIMO) technologies, enables to greatly improve the link reliability and increase the overall system capacity. For the design and test of such MIMO Mobile-to-Mobile systems, we need to have a thorough understanding and an accurate modelling of the underlying channels. For this purpose, the Geometrically-Based Stochastic Model (GBSM) has been applied for narrowband MIMO Mobile-to-Mobile channel modelling. The most important GBSMs include the one-ring model, two-ring model and Elliptical-ring model, in which the Elliptical-ring model is predestinated for modelling either narrow and wideband MIMO channels in microcellular and picocellular environments.

In this project, the statistical properties of narrowband MIMO Mobile-to-Mobile wireless fading channels in non-isotropic scattering environments will be investigated based on the elliptical-ring model. The interested properties include Space-Time (ST) Correlation (CF) properties, Space-Doppler-frequency (SD) Power Spectral Density (PSD), Level Crossing Rate (LCR), and Average Fading Duration (AFD).

I. Introduction

THE Multiple Input Multiple Output (MIMO) systems are equipped with multiple antennas, at both the transmitter and receiver in order to improve communication performance, in contrast to conventional communication systems with only one antenna on the transmitter and one antenna on the receiver.

MIMO is a method of transmitting and receiving two or more unique data streams through a single radio channel, increasing the maximum data rate achievable on every single radio channel.

By applying MIMO technology, we can directly take advantage of 2 very important properties; a. Diversity
b. Multiplexing.

Diversity means that the system provide a receiver with multiple replicas (copies) of the same information bearing signal, the duplicated signals are slightly changed by fading. The 3 types of Diversity techniques are:

i. Space Diversity

This means the antenna elements are sufficiently spaced apart to achieve independence between the transmitted and received signals. The spatial separation needs to be at least half the wavelength to obtain desired results of independence [1].

ii. Time Diversity – without wasting bandwidth

The same information is transmitted in different Time slots with the time slots separated by measures equal to or greater than the coherence time of the channel.

iii. Frequency Diversity

The same information is transmitted on different carrier frequencies which are separated by measures equal to or greater than the coherence bandwidth of the channel.

The reliability of the network is improved by taking advantage of the space and time diversity while the rate of transmission is improved by multiplexing.

MIMO can be used with any modulation or access technique, and it has been further improved by using a technique called Orthogonal Frequency Division Multiplexing (OFDM), through which we can divide the frequency selective channel into many flat fading channels and then apply the MIMO transmit/receive techniques to each of these sub-channels[2].

In Mobile-to-Mobile (M2M) communication channels, both the transmitter and the receiver are in motion. For example, one vehicle in a given location of a city tries to communicate to other moving vehicle in other location. This can be a police cars, emergency vehicles or military in certain an events.

In this situations were the vehicles are inside a city, the Line-of-Sight is often obstructed by buildings or any other type of obstacle between the transmitter and the receiver, these obstacles can be scatterers or any other mechanisms that diffract or reflect the signal.

A Mobile-to-Mobile propagation model is needed to evaluate mobile to mobile communication systems. The major difference between Mobile-to-Mobile and the Mobile-to-Base lies mainly in the location of the antennas, their heights and the surrounding scatterers. The proposed propagation model is based on a time variant channel.

The radio propagation channel determines crucial MIMO M2M system characteristics. Therefore the modelling of MIMO M2M channels plays the most important part for MIMO M2M system design, simulation and deployment. The modelling of a channel is an attempt to develop a mathematical model that describes a channel, the response to different input conditions, the behaviors, and determine its mathematical representation.

II. ELLIPTICAL MODEL

The MIMO M2M Elliptical Model is an example of a Geometric-Based Stochastic Model , and is preferred over the One-ring and Two-ring models, because while the latter models are used primarily to represent Narrow-band MIMO channels [3], the Elliptical model can be used to represent either narrow or wideband MIMO channels. The Frequency-selectivity feature of the Elliptical model also makes it the preferred choice for developers of future mobile communication systems [3].

The Geometric Elliptical model was originally proposed for spatial channels in micro and pico - cell environments, where the antenna heights are low, at ground level, so that multipath scattering is just as likely near the mobile station 1 as it is near the mobile station 2.

In the Elliptical Model, the MS1 and MS2 are closer to each other, and are placed at about the same vertical heights, and the scatterers exist on the ellipse surrounding both the MS1 and MS2, each positioned at the focal points of the Ellipse.

The Geometrical Elliptical Scattering Model has definitive properties which can be described by using its correlation functions. The correlation functions describe the basic components of the MIMO M2M communication system by its spatial, temporal and frequency characteristics. By analyzing the correlation functions is easier to investigate the potential of the MIMO M2M wireless communication systems.

In MIMO M2M channel modelling, it is important take into consideration the several issues that affect propagation within the channel like variation in time, multipath phenomena and Doppler shifts, angle of arrival of the received signals, and also the effects of using multiple carrier frequencies [4].

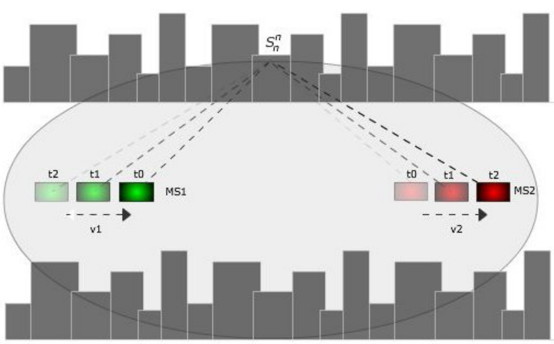

Fig.1. A MIMO M2M time variant channel based on the Elliptical-ring model.

The correlation between the frequency properties decreases when the frequencies or their differences increase. The proposed 3D model takes into account the antenna heights. The vertical separation of antenna elements is the result of their different heights. Such a difference in the antenna heights produces phase differences between the received or transmitted signals and consequently impact on the correlation function. This property can be employed to improve the space diversity in wireless systems [3].

In a MIMO M2M wireless system, the transmitted signal in the channel has a complicated interaction with the environment. There are reflections and refractions likely to occur from large objects, diffraction of the electromagnetic waves around objects, and signal scattering. The result of these complicated interactions is the presence of many signal components, differing paths of reception or multipath signals, at the receiver [5], which can be described using their Space, Time and Frequency properties.

Performing a correlation of these properties gives a more in-depth and accurate description of the MIMO M2M channel model, and I will start by reviewing the Space-Time Correlation properties, the Frequency Correlation properties, then the Space-Doppler-frequency Power Spectral Density, Level Crossing Rate and Average Fading Duration.

Previous work on this subject has proven that accurate models should take sufficient consideration of the physical geometry of scattering objects within the propagation environment, and under the coverage of both receiving and transmitting antennas [6] [7]. In this case, the scattering objects are assumed to lie along the ellipse, and the MS1 and MS2 are placed at the foci of the ellipse, as shown in the figure 1.

Due to Doppler Effect, if a transmitter is moving away from a receiver, the frequency of the received signal is lower than the one sent out from the transmitter; otherwise, the frequency is increased. In wireless communications, there are many factors that can cause relative movement between a transmitter and a receiver. It can be the movement of a mobile or it can be the movement of some objects in the background that causes the change of path length between the transmitter and the receiver. The lengths of signal path are often different, which correspond to different movement speeds of transmitter signals, and in turn different frequency shifts on the signal paths. As a result, a frequency spread is caused in the signal spectrum.

The energy spectral density describes how the energy (or variance) of a signal is distributed with frequency.

The Level Crossing Rate and Average Fading Duration are two important second order statistics that make the Mobile-to-Mobile channels significantly different from Fixed-to-Mobile (F2M) channels.

The Level Crossing Rate is a measure of the rapidity of the fading. It quantifies how often the fading crosses some threshold, usually in the positive-going direction.

The average fade duration quantifies how long the signal spends below the threshold.

As the amplitude of a signal received over such a channel also fluctuates, the receiver will experience periods during which the signal can not be recovered reliably. If a certain minimum (threshold) signal level is needed for acceptable communication performance, the received signal will experience periods of:

- Sufficient signal strength or "non-fade intervals", during which the receiver can work reliably and at low bit error rate.
- Insufficient signal strength or "fades", during which the bit error rate inevitably is close to one half (randomly guessing ones and zeros) and the receiver may even fall out of lock.

Channel fading occurs mainly because the user moves. If the user is stationary almost no time variations of the channel occur (except if reflecting elements in the environment move).

III. A MATHEMATICAL REPRESENTATION OF THE MIMO M2M GEOMETRIC ELLIPTICAL MODEL

The Elliptical Scattering Model describes a system where the two mobile stations MS1 and MS2 are located at the focal points of the ellipse, these mobile stations are described as a vectors, each with magnitude (speed V_T and V_R) and direction (angles of motion γ_T and γ_R) [8].

The circumference of the ellipse describe all the local effective scatterers $S_{TR}^{(n)}$ associated with the Angles of Departure of the waves bounced and designated by $\phi_T^{(n)}$, this waves travel the distance $\xi_T^{(n)} + \xi_R^{(n)} = 2a$.

The major axis is denoted by 'a' and the minor axis of the ellipse is the denoted by 'b'.

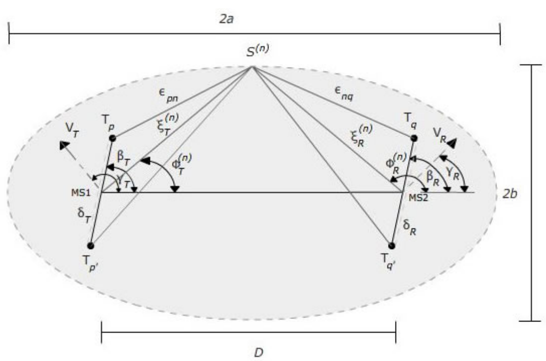

Fig.2. Geometric Elliptical Scattering model for a MIMO M2M channel with local scatterers S(n) lying on an ellipse.

Here, we assume that both the MS1 and MS2 are able to receive and transmit information. In this case the MS1 will be the transmitter and MS2 will be the receiver, these two stations are equipped with a uniform linear antenna array consisting of MT and MR antenna elements respectively.

The angles shown in the figure 2 represent the tilt angles of the Transmit (β_T) and Receive (β_R) antenna arrays, the Angle of Departure and the Angle of Arrival. The antenna element distance (spacing) δ_T at Tx and δ_R at Rx.

A few assumptions were made while resolving these equations and they are stated as we proceed.

The received signal is constructed as a sum of the Line of Sight and Single Bounced rays with different energies.

Consider in this MIMO M2M Elliptical ring model with Single Bounced rays the distance (D) between the Tx and Rx, the number of effective scatterers (N) lie on an ellipse with Tx and Rx located at the foci.

The received complex impulse response for $T_p - R_q$ link is a superposition of the LoS and Single Bounced rays.

$$h_{pq}(t) = h_{pq}^{LoS}(t) + h_{pq}^{EL}(t) \tag{1}$$

$$h_{pq}^{LoS}(t) = \sqrt{\frac{K_{pq}\Omega_{pq}}{K_{pq}+1}} e^{-j2\pi f_c \tau_{pq}} \times e^{j\left[2\pi f_{T\max} t \cos\left(\pi - \phi_{Rq}^{LoS} + \gamma_T\right) + 2\pi f_{R\max} t \cos\left(\phi_{Rq}^{LoS} + \gamma_R\right)\right]} \tag{2}$$

$$h_{pq}^{EL}(t) = \sqrt{\frac{\Omega_{pq}}{K_{pq}+1}} \lim_{N\to 0} \sum_{n=1}^{N} \frac{1}{\sqrt{N}} e^{j\left(\psi_n - 2\pi f_c \tau_{pq,n}\right)} \tag{3}$$

where $p = 1, 2, ..., M_T$ and $q = 1, 2, ..., M_R$.

The Time delay between the p^{th} MS1 and q^{th} MS2 antenna elements as described in the elliptical figure 3.1 can be deduced by dividing the distances by the speed of light, c, the wave propagation velocity $\tau_{pq} = \frac{\varepsilon_{pq}}{c}$.

The travel times of the waves through the link $T_p - R_q$

$$\tau_{pq,n} = \frac{\left(\varepsilon_{pn} + \varepsilon_{nq}\right)}{c} \tag{4}$$

where c is the speed of light, K_{pq} is the Ricean factor, Ω_{pq} is the total power transferred through of $T_p - R_q$ link, the Maximum Doppler frequencies associated with the Tx $f_{T\max} -> \frac{V_T}{\lambda}$ and Rx $f_{R\max} -> \frac{V_R}{\lambda}$.

The distances between the Transmitter and the Receiver antennas to the scatterers along the ellipse, can be expressed in terms of the antenna element spacing, the Angle of Arrival and the Angle of Departure. Distances ε_{pq} can be expressed as functions of the relevant angles.

Assuming $D >> \{\delta_T, \delta_R\}$ and using the laws of cosines and sines, the distances can be calculated as follows.

For the Line of Sight (LoS)

$$\varepsilon_{pq} \approx \varepsilon - K_q \delta_R \cos\left(\phi_{Rq}^{Los} - \beta_R\right) \tag{5}$$

$$\varepsilon \approx D - K_q \delta_T \cos \beta_T \tag{6}$$

For macro and micro-cell scenarios where

$D >> \max\{R_T, R_R\}$

$$\phi_{Rq}^{LoS} \approx \pi \quad (7)$$

For pico-cell scenarios where $D >> \max\{R_T, R_R\}$ is not fulfilled

$$\phi_{Rq}^{LoS} \approx \pi - \frac{K_p \delta_T \sin\beta_T}{D} \quad (8)$$

$$K_p = \frac{(M_T - 2p + 1)}{2} \quad (9)$$

$$K_q = \frac{(M_R - 2q + 1)}{2} \quad (10)$$

For the Single-bounced component of the Elliptical-ring model

$$\varepsilon_{pn} \approx \xi_T^n - K_p \delta_T \cos\left(\phi_T^{(n)} - \beta_T\right) \quad (11)$$

$$\varepsilon_{nq} \approx \xi_R^n - K_q \delta_R \cos\left(\phi_R^{(n)} - \beta_R\right) \quad (12)$$

where

$$\xi_T^{(n)} = \frac{a^2 + \frac{D^2}{4} + aD\cos\phi_R^{(n)}}{a + \frac{D\cos\phi_R^{(n)}}{2}} \quad (13)$$

$$\xi_R^{(n)} = \frac{b^2}{a + \frac{D\cos\phi_R^{(n)}}{2}} \quad (14)$$

In order to reduce the computational complexity we use a new exact and simple relationship between the AoA and AoD for the MIMO M2M Elliptical ring model to replace the previous approximate relationship in [9]. Consider $f = D/2$, based on the application of the law of cosines and sines in the triangle $O_T S_T^{(n)} O_R$ from figure 2, we obtain $\left(\xi_T^{(n)}\right)^2 = \left(\xi_R^{(n)}\right)^2 + 4f^2 + 4f\xi_R^{(n)}\cos\phi_R^{(n)}$ and $\left(\xi_T^{(n)}\right)/\sin\phi_R^{(n)} = \left(\xi_R^{(n)}\right)/\sin\phi_T^{(n)}$, respectively.

Here $\xi_T^{(n)} + \xi_R^{(n)} = 2a$, the exact relationship between the AoA and AoD as

$$\sin\phi_T^{(n)} = \frac{b^2 \sin\phi_R^{(n)}}{a^2 + f^2 + 2af\cos\phi_R^{(n)}} \quad (15)$$

$$\cos\phi_T^{(n)} = \frac{2af + \left(a^2 + f^2\right)\cos\phi_R^{(n)}}{a^2 + f^2 + 2af\cos\phi_R^{(n)}} \quad (16)$$

In order to characterize the AoD $\phi_T^{(n_i)}$ and AoA $\phi_R^{(n_i)}$, we use the von Mises PDF defined as $f(\phi) \triangleq \exp\left[k\cos(\phi - \mu)\right]/2\pi I_0(k)$, where $\phi \in [-\pi, \pi], I_0(\cdot)$ is the zero order modified Bessel function of the first kind, $\mu \in [-\pi, \pi]$ accounts for the mean value of the angle ϕ, and $k(k \geq 0)$ is a real valued parameter that controls the angle spread of the angle ϕ [8].

The normalized ST CF between any two complex impulse responses $h_{pq}(t)$ and $h_{p'q'}^{\dagger}(t)$ is defined as

$$\rho_{h_{pq}h_{p'q'}}(\tau) = \frac{\mathrm{E}\left[h_{pq}(t)\,h_{p'q'}(t+\tau)^*\right]}{\sqrt{\mathrm{E}\left[\left|h_{pq}(t)\right|^2\right]E\left[\left|h_{p'q'}(t)\right|^2\right]}} \quad (17)$$

where $(\cdot)^*$ denotes the complex conjugate operation, $\mathrm{E}[\cdot]$ is the statistical expectation operator, $p, p' \in \{1, 2, ..., M_T\}$ and $q, q' \in \{1, 2, ..., M_R\}$. This is a function of time separation τ and antenna elements spacing δ_T and δ_R.

Using trigonometric transformations

$$\int_{-\pi}^{\pi} \exp(a \times \sin c + b\cos c) = 2\pi I_0\left(\sqrt{a^2 + b^2}\right)$$

In the case of LoS component,

$$\rho_{h_{pq}^{LoS}h_{p'q'}^{LoS}}(\tau) = \sqrt{K_{pq}K_{p'q'}}\, e^{j2\pi G - j2\pi\tau H} \quad (18)$$

Where for macro – micro – cell scenarios

$$G = P\cos\beta_T - Q\cos\beta_R \quad (19)$$

$$H = f_{T\max}\cos\gamma_T - f_{R\max}\cos\gamma_R \quad (20)$$

and for pico – cell scenarios

$$G = P\cos\beta_T - Q\cos\beta_R + \frac{\sin\beta_T \sin\beta_R\left(P(M_R+1)\delta_R + Q(M_T+1)\delta_T - 2U\right)}{2D} \quad (21)$$

$$H = f_{T\max}\left(\cos\gamma_T + \frac{K_{p'}\delta_T \sin\beta_T \sin\gamma_T}{D}\right) - f_{R\max}\left(K_{p'}\delta_T \times \sin\beta_T \sin\gamma_R - \frac{\cos\gamma_R}{D}\right) \quad (22)$$

$$P = (p' - p)\,\delta_T / \lambda \quad (23)$$

$$Q = (q' - q)\,\delta_R / \lambda \quad (24)$$

$$U = (p'q' - pq)\,\delta_T\delta_R / \lambda \quad (25)$$

$$K_{p'} = (M_T - 2p' + 1)/2 \quad (26)$$

$$K_{q'} = (M_R - 2q' + 1)/2 \quad (27)$$

The single bounced component of the elliptical-ring model.

$$\rho_{h_{pq}^{EL}h_{p'q'}^{EL}}(\tau)=\frac{n_{SB}}{2\pi I_0\left(K_R^{SB}\right)}\int_{-\pi}^{\pi}e^{J+j2\pi(T-\tau V)} \quad (28)$$

non-isotropic

$$J=K_R^{SB}\cos\left(\phi_R^{SB}-\mu_R^{SB}\right) \quad (29)$$

Space

$$T=P\cos\left(\phi_T^{SB}-\beta_T\right)+Q\cos\left(\phi_R^{SB}-\beta_R\right) \quad (30)$$

Time

$$V=f_{T\max}\cos\left(\phi_T^{SB}-\gamma_T\right)+ f_{R\max}\cos\left(\phi_R^{SB}-\gamma_R\right) \quad (31)$$

where

μ_R^{SB} is the mean value of AoA ϕ_R^{SB}.

K_R^{SB} controls the angle spread of the AoA ϕ_R^{SB}.

Applying the Fourier transformation in terms of time to the ST CF, we obtain

$$F\left\{\rho_{h_{pq}h_{p'q'}}(\tau)\right\}=\int_{-\infty}^{\infty}\rho_{h_{pq}h_{p'q'}}(\tau)e^{-j2\pi f_{D}\tau}d\tau \quad (32)$$

where f_D is the Doppler frequency.

In the case of the LoS components

$$F\left\{\rho_{h_{pq}^{LoS}h_{p'q'}^{LoS}}(\tau)\right\}=\sqrt{K_{pq}K_{p'q'}}e^{j2\pi G}\delta\left(f_D+H\right)$$

where $\delta(\cdot)$ denotes the Dirac delta function.

In the case of single bounced component of the elliptical-ring model we must evaluate the integral in (32).

Based on the introduced channel model, I will derive the LCR and AFD for a non-isotropic scattering environment. First need to be defined the appropriate time autocorrelation function (ACF) and the notion of spectral moments, which are fundamentals of further deriving the LCR and AFD in this section. The ACF of the complex impulse response of diffuse component $h_{pq}^{DIF}(t)$ is defined as $\rho_{h_{pq}^{DIF}}(\tau)=\mathrm{E}\left[h_{pq}^{DIF}(t)h_{pq}^{DIF*}(t+\tau)\right]$, where $(\cdot)^*$ denotes the complex conjugate operation, $\mathrm{E}[\cdot]$ is the statistical expectation operator. It is shown in (5) that based on the application of the von Mises PDF and trigonometric transformations, the time ACF of single bounced components are given by

$$\rho_{h_{pq}^{EL}}(\tau)=\frac{n_{SB}\Omega_{pq}}{2\pi\left(K_{pq}+1\right)I_0\left(K_R^{SB}\right)}\int_{-\pi}^{\pi}e^{J-j2\pi\tau V}d\phi_R^{SB} \quad (33)$$

where $J=k_R^{SB}\cos\left(\phi_R^{SB}-\mu_R^{SB}\right)$,

$V=f_{T\max}\cos\left(\phi_T^{SB}-\gamma_T\right)+f_{R\max}\cos\left(\phi_R^{SB}-\gamma_R\right)$,

with $\phi_T^{SB}\left(\phi_R^{SB}\right)$ being the continuous notations of $\phi_T^{(n)}\left(\phi_R^{(n)}\right)$.

The n^{th} spectral moment, $b_n\left(n=0,1,2,...,\right)$, is defined to be $b_n=\left.\frac{d^n\rho_{pq}^{DIF}(\tau)}{2j^n d\tau^n}\right|_{\tau=0}$, where $j^2=-1$. Based on the application of the von Mises PDF, the spectral moments b_1^{SB} and b_2^{SB} for the single bounced component can be derived by successive differentiation of

$$b_1^{SB}=-b_0^{SB}\int_{-\pi}^{\pi}\frac{e^{kR\cos\left(\phi_R^{SB}-\mu_R\right)}L_R}{I_0\left(k_R\right)}d\phi_R^{SB} \quad (34)$$

$$b_2^{SB}=b_0^{SB}\int_{-\pi}^{\pi}\frac{2\pi e^{kR\cos\left(\phi_R^{SB}-\mu_R\right)}L_R^2}{I_0\left(k_R\right)}d\phi_R^{SB} \quad (35)$$

where

$L_R=f_{T\max}\cos\left(\phi_T^{SB}-\gamma_T\right)+f_{R\max}\cos\left(\phi_R^{SB}-\gamma_R\right)$,

$b_0^{SB}=\frac{n_{SB}\Omega_{pq}}{2\left(K_{pq}+1\right)}$.

For a fading signal, the LCR $N_R\left(r_n\right)$, is by definition the average number of times per second that the single envelope, $R(t)=\left|h_{pq}(t)\right|$, crosses a specified level r_n with positive/negative slope.

The AFD, $T_R-\left(r_n\right)$, is the average time over which the signal envelope, $R(t)$, remains below certain level r_n. In general, the AFD $T_R-\left(r_n\right)$ is defined by [8].

$$T_R-\left(r_n\right)=\frac{P_R-\left(r_n\right)}{N_R\left(r_n\right)} \quad (36)$$

where $P_R-\left(r_n\right)=1-Q\left(\sqrt{2K_{pq}}\sqrt{2\left(K_{pq}+1\right)}r_n\right)$ indicates a cumulative distribution function of $R(t)$ with $Q(\cdot,\cdot)$ denoting the generalized Marcum Q function.

IV. Numerical Results and Analyses

The parameters used for this numerical analysis:

$f_c=5.9GHz, f_{T\max}=f_{R\max}=570Hz, \beta_T=\pi/3, \beta_R=\pi/4, a=250m, D=350m$

$\gamma_T=0, \gamma_R=\pi, K_T=0, K_R=0, \mu_T=0, \mu_R=\pi, K_{pq}=5$

The spectral shape of the Doppler spread determines the time domain fading waveform and dictates the temporal correlation and fade slope behaviors.

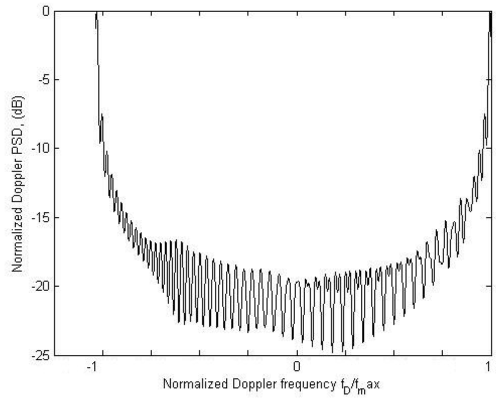

Fig.3. SD PSD $k_T = k_R = 0, \gamma_T = 0, \gamma_R = \pi$ opposite direction in isotropic scattering environment.

Normalized LCR and AFD of the MIMO M2M model for different Ricean factors $k_{pq} = 0, k_{pq} = 1, k_{pq} = 5$ and $(k_T = k_R = 1, \gamma_T = 0, \gamma_R = \pi)$.

The influence of the Ricean factor k_{pq} and ratio factor s (s is the ratio of the maximum Doppler frequency $f_{R\max}$ and $f_{T\max}$, $s = f_{R\max} / f_{T\max}$) for a non-isotropic M2M channel on the LCR and AFD. The fades are shallower when k_{pq} is larger or s is smaller. Furthermore, the AFD tends to be larger when k_{pq} is larger or s is smaller.

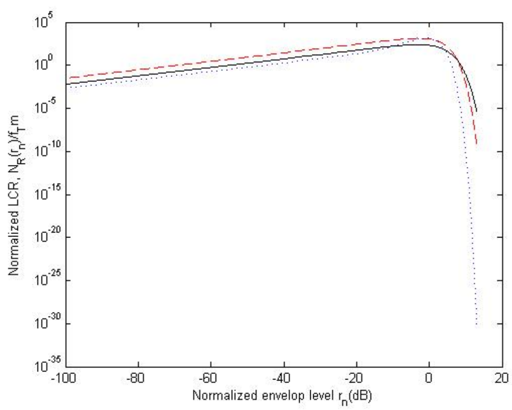

Fig.4. LCR $k_{pq} = 0$ (black) $k_{pq} = 1$ (red) $k_{pq} = 5$ (blue) in non isotropic scattering environment.

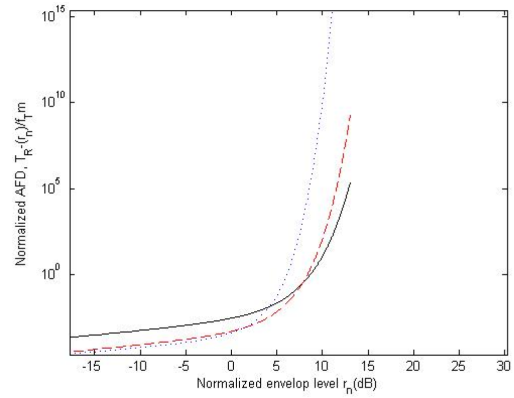

Fig.5. AFD $k_{pq} = 0$ (black) $k_{pq} = 1$ (red) $k_{pq} = 5$ (blue) in non isotropic scattering environment.

V. Conclusion

In this study, the influence of the different physical parameters that determine a Multiple Input Multiple Output (MIMO) Mobile to Mobile (M2M) Elliptical ring channel were mathematically modeled and analyzed.

In this study, in order to test and analyze the Statistical properties of the mathematical model, a GUI - Simulation Environment was developed for the MIMO M2M Elliptical ring model.

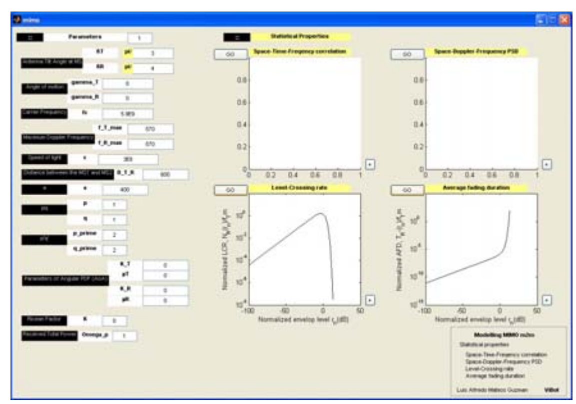

Fig.6. MIMO M2M Elliptical ring Simulator.

The ST CF and the corresponding SD PSD for 2D non isotropic scattering environments are derived. Based on the obtained Doppler PSD for the elliptical ring model with single bounced rays and observations in [8], can be conclude that no matter what the propagation environment is, for M2M channels in non isotropic scattering environments, the single bounced rays will cause a Doppler PSD similar to the U shape.

The second order statistics of the non-isotropic MIMO M2M Ricean fading channel are considered and the analytical expressions for the LCR and AFD have been derived. Based on the derived LCR and AFD some important parameters were investigated in more detail.

The numerical simulations have revealed that the LCR and AFD are very sensitive to the angle spreads $\left(K_T^{SB}, K_R^{SB}\right)$, mean values $\left(\mu_T^{SB}, \mu_R^{SB}\right)$ of the AoA ϕ_R^{SB} and AoD ϕ_T^{SB}, and directions of motion (γ_T and γ_R) in non-isotropic scattering environments.

APPENDIX

http://www.amcomputersystems.com/vibot/vibots/mateos/index.html.

ACKNOWLEDGMENT

My grateful thanks to my supervisor, Dr Cheng-Xiang Wang, for his support throughout this research project and to MSc Xiang Cheng whose generous suggestions helped make changes and improvements in this project

REFERENCES

[1] A. Constantinides, and A. Shacham, “MIMO Wireless Systems”, May 14 2004,http://www.columbia.edu/~acc40/MIMO.pdf.

[2] K. Ebruke, "A study on geometrially-based stochastic MIMO channel models," Master thesis, 2007. H.

[3] Matthias P¨atzold and Bjørn Olav Hogstad, “A Wideband MIMO Channel Model Derived From the Geometric Elliptical Scattering Model,” Proc. 3rd International Symposium on Wireless Communication System, ISWCS'06, Valencia, Spain, Sept. 2006, pp. 138–143.E..

[4] P. Almers, and E. Bonek, etc., “Survey of Channel and Radio Propagation Models for Wireless MIMO Systems,” EURASIP Journal on Wireless Communications and Networking, vol. 2007, pp. 1–19, 2007.

[5] A. S. Akki, “Statistical properties of mobile-to-mobile land communication channels,” IEEE Trans. Veh. Technol., vol. 43, no. 4, pp. 826–831, Nov. 1994.

[6] A. S. Akki and F. Haber, “A statistical model for mobile-to-mobile land communication channel,” IEEE Trans. Veh. Technol., vol. VT-35, no. 1, pp. 2–7, Feb. 1986.

[7] Gordon L. Stüber, “Principles of Mobile Communication”, 2nd edition, Kluwer Academic Publishers, Boston, 2001. Chapter 2: Propagation modelling.

[8] X. Cheng, C.-X. Wang, and D. I. Laurenson, “A generic geometrical-based MIMO mobile-to-mobile channel model,” IEEE IWCMC’08, Chania Crete Island, Greece, submitted for publication.

[9] X. Cheng, C.-X. Wang, and D. I. Laurenson, “Space-time-frequency characterization of non-isotropic MIMO mobile-to-mobile multicarrier Ricean fading channels,” IEEE IWCMC’08, Chania Crete Island, Greece, submitted for publication.